ChemComm

COMMUNICATION

View Article Online
View Journal | View Issue

Cite this: *Chem. Commun.*, 2020, **56**, 15623

Received 1st September 2020,
Accepted 19th November 2020

DOI: 10.1039/d0cc05837h

rsc.li/chemcomm

Reaction between Ag_{17}^+ and acetylene outside the mass spectrometer: dehydrogenation in the gas phase†

Madhuri Jash, Rabin Rajan J. Methikkalam, Mohammad Bodiuzzaman, Ganesan Paramasivam and Thalappil Pradeep *

We present the first example of acetylide protected silver clusters by a reaction between Ag_{17}^+ and acetylene, conducted around atmospheric pressure. The products were obtained after dehydrogenation of acetylene in the gas phase. The observed reaction mechanism may be helpful to design new catalysts useful in organometallic chemistry.

Atomically precise nanoclusters (NCs), being the link between atoms and bulk materials, show unique properties and represent one of the major pillars of current nanoscience.[1] Due to their electronic and geometric shell closing and quantum confinement, even a change of one atom can alter their physical and chemical properties.[2] Catalytic properties of most of the NCs are studied in the supported form after ligand desorption, although stabilizing clusters after ligand removal, in a specific size and shape, is of concern.[3] In contrast, gas phase studies of size-selected naked clusters give us molecular level understanding of their catalytic processes due to the absence of ligands and the stabilising medium.[4–6]

From an organometallic point of view, transition metal–π complexes are crucial intermediates of several metal-mediated transformations.[7,8] This kind of metal-unsaturated hydrocarbon interaction can be varied by changing a single metal atom in a metal cluster.[4,9] The type of interaction can be ionic, covalent or weak ion–π interaction, depending on the cluster's atomicity, valence electrons and ligands. Mass spectrometry,[10] photoelectron spectroscopy[11] and infrared spectroscopy[12] are different characterization tools for the investigation of such gas phase interactions along with quantum chemical calculations.

Gas phase reactivity and catalysis of cluster metal ions have been reported by various research groups, inside the mass spectrometer.[4,5,13,14] The first report of the formation of silver clusters by electrospray ionization under atmospheric pressure was in 2013.[15] Later, we had shown that single gas phase species, Ag_{17}^+ can be produced outside as well as inside a mass spectrometer, without mass selection.[16,17] Recently, it has also been shown that Ag_{17}^+ reacts with acetylene under vacuum and formed $-C_2H_5$ attached Ag_{17}^+ within the ion trap.[18] However, interaction of such large sized clusters has not been studied before outside the mass spectrometer, under atmospheric pressure conditions. In this communication, we explored the interaction of acetylene with Ag_{17}^+ outside a mass spectrometer where Ag_{17}^+ forms adducts with 2, 4 and 6 acetylene molecules after dehydrogenation. Density functional theory (DFT) calculations elucidate the structure of these adducts along with the dehydrogenation mechanism.

Gas phase ion–molecule reaction experiments were conducted using a LTQ XL Linear Ion Trap Mass Spectrometer with an external home-built nano-electrospray ion source. Here, we have used $[Ag_{18}H_{16}(TPP)_{10}]^{2+}$ clusters as a precursor analyte, which was synthesized following a reported method[19] and details are presented in the Experimental section. All the characteristic features including their UV-Vis spectrum, high resolution ESI mass spectrum and formation of deuterated analogue, $[Ag_{18}D_{16}(TPP)_{10}]^{2+}$ (measured with a Synapt G2Si HDMS instrument) confirm the formation of the cluster and all these data are shown in Fig. S1A–D (ESI†). The electrosprayed cluster was passed through a heating tube by using N_2 as the nebulizing gas to obtain a stream of the naked cluster. This flow of naked cluster ions was reacted with acetylene outside the mass spectrometer. Fig. 1 shows a schematic of the experimental set-up which consists of a coiled copper tube as the heater, a stainless steel union cross connector with external gas line and an LTQ mass spectrometer. Formation of naked clusters from $[Ag_{18}H_{16}(TPP)_{10}]^{2+}$ was presented in our previous report.[16] The end of the heating tube was connected to one inlet of the union cross connector. Another inlet was fixed to the acetylene gas channel, an outlet was directed to the mass spectrometer inlet and another port was blanked. The acetylene gas channel was made with a stainless-steel tube of 1.5 mm

DST Unit of Nanoscience (DST UNS) and Thematic Unit of Excellence (TUE), Department of Chemistry, Indian Institute of Technology Madras, Chennai 600 036, India. E-mail: pradeep@iitm.ac.in

† Electronic supplementary information (ESI) available. See DOI: 10.1039/d0cc05837h

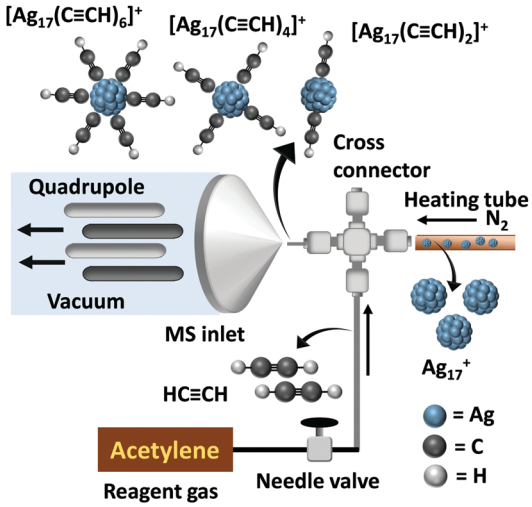

Fig. 1 Schematic diagram for an ion/molecule reaction between naked clusters and acetylene. Acetylene was crossed with the flowing naked clusters coming out from the heating tube and the products are detected with an LTQ mass spectrometer.

outer diameter and 0.7 mm inner diameter, where the gas flow could be controlled with a needle valve. This set-up was kept in air, to make ion/molecule reactions feasible in air. The resulting ions, coming out from the cross connector enter the transfer capillary of the mass spectrometer and are analysed by the LTQ mass spectrometer.

At first, naked clusters were made from electrosprayed $[Ag_{18}H_{16}(TPP)_{10}]^{2+}$ in the absence of acetylene and the ESI mass spectrum obtained is shown in Fig. 2A. During this process, we get Ag_{17}^{+} (m/z 1833) and $Ag_{18}H^{+}$ (m/z 1943) alone, without any mass selection. To study the ion/molecule reaction under ambient conditions, acetylene gas (from Rana Industrial Gases & Products, purity 99.99%) was introduced into the cross connector where the naked clusters enter from the heating tube along with N_2. During this reaction, the N_2 gas flow was increased from 25 psi to 40 psi to obtain adequate ion signal in the mass spectrometer. Fig. 2B represents the ESI mass spectrum after introducing acetylene gas at a lower flow rate. Three adduct peaks of $[Ag_{17}(C{\equiv}CH)_2]^{+}$, $[Ag_{17}(C{\equiv}CH)_4]^{+}$ and $[Ag_{17}(C{\equiv}CH)_6]^{+}$ appeared at m/z 1883, 1933 and 1983, respectively and the intensity of Ag_{17}^{+} got reduced. The isotopic distributions of Ag_{17}^{+} and the adducts matched well with their calculated spectra shown in Fig. S2 (ESI†). As acetylene pressure was increased in Fig. 2C, the intensities of the adduct peaks increased and the peak of Ag_{17}^{+} disappeared. Dehydrogenation of acetylene (C_2H_2) to acetylide ($-C_2H$) during adduct formation was confirmed by the mass shift of $\Delta m/z$ = 2, 4 and 6 in the case of $[Ag_{17}(C{\equiv}CH)_2]^{+}$, $[Ag_{17}(C{\equiv}CH)_4]^{+}$ and $[Ag_{17}(C{\equiv}CH)_6]^{+}$, respectively (Fig. 2D–F). As always even mass shift was seen, which was suggested to be due to the loss of a hydrogen molecule (H_2) during adduct formation, in our experimental conditions. Here the disappearance of $Ag_{18}H^{+}$ with acetylene gas flow can be due to its very low abundance. Full range ESI mass spectra of this ion/molecule reaction are shown in Fig. S3 (ESI†). The reaction of $Ag_{17}H_{14}^{+}$ was also conducted with acetylene, but it was inert due to the surface passivation by hydride ligands.

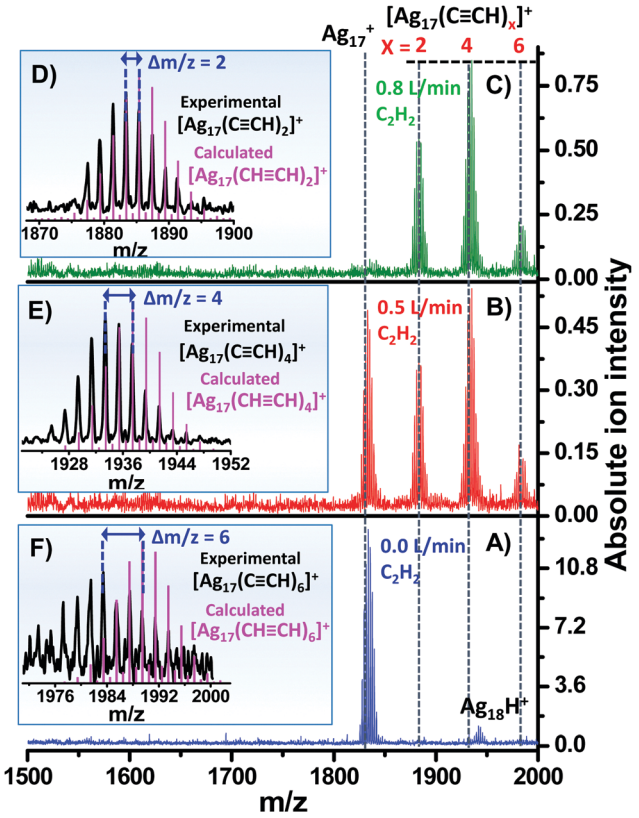

Fig. 2 (A) ESI mass spectrum of Ag_{17}^{+} and $Ag_{18}H^{+}$ before the reaction with acetylene. (B and C) Are the ESI mass spectra after the reaction between Ag_{17}^{+} and acetylene, at different flow rates of acetylene. During this reaction, three adducts appeared as $[Ag_{17}(C{\equiv}CH)_2]^{+}$, $[Ag_{17}(C{\equiv}CH)_4]^{+}$ and $[Ag_{17}(C{\equiv}CH)_6]^{+}$. The experimental (black) spectrum of (D) $[Ag_{17}(C{\equiv}CH)_2]^{+}$, (E) $[Ag_{17}(C{\equiv}CH)_4]^{+}$ and (F) $[Ag_{17}(C{\equiv}CH)_6]^{+}$ show mass shifts of $\Delta m/z$ = 2, 4, 6 with the calculated spectrum (magenta) of $[Ag_{17}(CH{\equiv}CH)_2]^{+}$, $[Ag_{17}(CH{\equiv}CH)_4]^{+}$ and $[Ag_{17}(CH{\equiv}CH)_6]^{+}$, respectively.

To get a clear idea about the structure and binding pattern of the adducts, collision induced dissociation (CID) experiments were performed. For a simpler representation, the adducts $[Ag_{17}(C{\equiv}CH)_2]^{+}$, $[Ag_{17}(C{\equiv}CH)_4]^{+}$ and $[Ag_{17}(C{\equiv}CH)_6]^{+}$ are denoted as (17,2), (17,4) and (17,6), respectively where the first number inside the bracket represents the atomicity of the silver core and the second number represents the number of acetylide ligands attached to it. The same notation is also followed for the CID fragments. Here all the adducts and their CID fragments are in +1 charge states which is not mentioned separately in the case of bracket notations. The fragmentation patterns (MS^2 and MS^3) of (17,2) are shown in Fig. 3A with two concentric rings. The full fragmentation patterns from MS^2 to MS^6 are shown as a flow chart and also in the form of five concentric rings in Fig. S4A and B (ESI†), respectively. In Fig. 3A, the inner ring, closer to the centre, shows the five different MS^2 fragments of (17,2). The MS^2 spectrum showing these fragmented peaks is given at the centre of that circle. Then, the next level fragmentation is shown in a lighter shade of the same colour. Here the second ring represents the MS^3 fragmentation products of the five MS^2 fragments. Fig. 3B–F are the MS^3 spectra of (17,1), (16,2), (16,1), (15,2) and (15,0), respectively. As it was not possible to represent all the

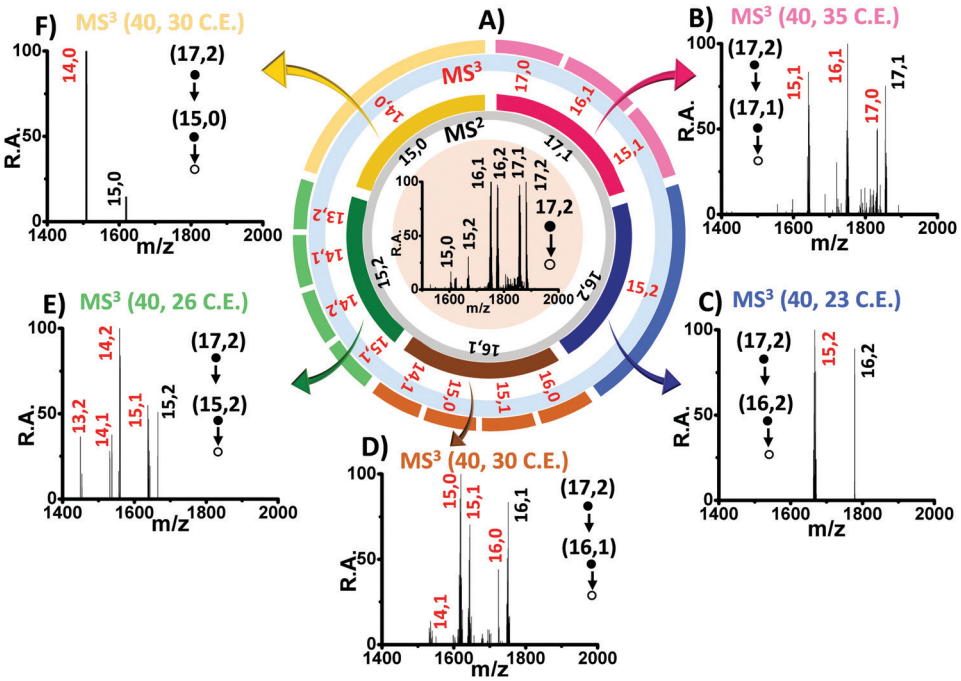

Fig. 3 The CID fragments of $[Ag_{17}(C{\equiv}CH)_2]^+$ or (17,2) resulting from MS^2 and MS^3 experiments. (A) represents the MS^2 spectrum of (17,2) at the centre of the circle and the MS^2 and MS^3 fragments with two individual concentric rings. (B–F) represent the MS^3 spectrum of the corresponding (17,1), (16,2), (16,1), (15,2) and (15,0) fragments, respectively. The collision energies used are mentioned as MS^3 (*xx*, *yy* C.E.) corresponding to MS^2 and MS^3 data and are in an instrumental unit.

mass spectra up to MS^6 level in a single figure, we have plotted them separately. The different fragmentation pathways of (17,2), which proceed through (17,1), (16,2), (16,1) and (15,2) in MS^3 level are presented in Fig. S5–S9 (ESI†). Whereas, the ion (15,0) does not reveal any fragmentation, probably due to low intensity.

For the (17,4) adduct, the overall fragmentation flowchart is shown in Fig. S10A (ESI†). In Fig. S10B (ESI†), the same fragmentation data are shown with two concentric rings. Fig. S11A (ESI†) shows the MS^2 mass spectrum of (17,4) with three fragments, (17,3), (17,0) and (16,3). Fig. S11B–D (ESI†) are the MS^3 mass spectra of (17,3), (17,0) and (16,3), respectively. For the third adduct (17,6), Fig. S12A (ESI†) represents the fragmentation flowchart whereas Fig. S12B (ESI†) represents it with one ring of MS^2 fragments. The MS^2 mass spectrum of (17,6) is shown in Fig. S13 (ESI†) with seven fragments. From all the fragmentation patterns of the three adducts, it is noticed that during the fragmentation process, the acetylide ligand can get knocked out from the cluster core with or without the silver atom. This result is very much unlike that from our previous report, fragmentation of the oxygen added peaks of Ag_{17}^+.[16] During the CID of oxygen added peaks, there was at first detachment of all oxygen atoms (ligands), forming intact Ag_{17}^+, which was further fragmented to smaller silver naked clusters with higher collision energy. From this result, we conclude that the fragmentation pattern of Ag_{17}^+ adducts depends on the binding type of silver with the ligand. The experimental and calculated masses of all the assigned clusters in this experiment are summarized in Table S14 (ESI†).

The structures of Ag_{17}^+ and adducts were optimised using density functional theory. The structure of Ag_{17}^+ was optimized based on a previously reported method and then it was used for further calculations.[20] The most stable structures of Ag_{17}^+ and its adducts are shown in Fig. S15 (ESI†). In Fig. S16 (ESI†), their HOMO–LUMO gaps are also given. During the reaction, the increases in mass of the three adduct peaks were *m*/*z* 50, 100 and 150 which are due to 2, 4 and 6 $-C_2H$ additions and desorption of 1, 2 and 3 hydrogen molecules, respectively as below:

$$Ag_{17}^+ + 2C_2H_2 \rightarrow [Ag_{17}(C{\equiv}CH)_2]^+ + H_2\uparrow$$
$$Ag_{17}^+ + 4C_2H_2 \rightarrow [Ag_{17}(C{\equiv}CH)_4]^+ + 2H_2\uparrow$$
$$Ag_{17}^+ + 6C_2H_2 \rightarrow [Ag_{17}(C{\equiv}CH)_6]^+ + 3H_2\uparrow$$

To determine the actual mechanism of dehydrogenation, initially the interaction was calculated with one and two intact acetylene molecules over Ag_{17}^+, which show weak non-covalent cluster–π interactions (Fig. S17, ESI†). According to a previous report, the dissociation threshold values for such larger cluster–π moieties (for Ag_n^+, when $n > 7$) is small, which makes them sufficiently unstable.[21] However, for $[Ag_{17}(HC{\equiv}CH)_2]^+$, due to dehydrogenation of two acetylene molecules, we may have either one butadiyne ($-C_4H_2$) or two acetylide ($-C_2H$) attached Ag_{17}^+ (Fig. S18, ESI†). The calculated total energies of these two structures are closer to each other but the binding energy values show that in $[Ag_{17}(C{\equiv}CH)_2]^+$, the interaction of C_2H units with silver are stronger (covalent) than the butadiyne unit in $[Ag_{17}C_4H_2]^+$ (non-covalent). Hence, the $[Ag_{17}(C{\equiv}CH)_2]^+$ structure, where the average bond distance of Ag–C was 2.25 Å, was considered for further calculation.

Possible mechanism for the formation of a hydrogen molecule after dehydrogenation of an even number of acetylenes interacting with Ag_{17}^+, was studied in detail. Fig. 4 shows the energy profile during the dehydrogenation of two acetylene over

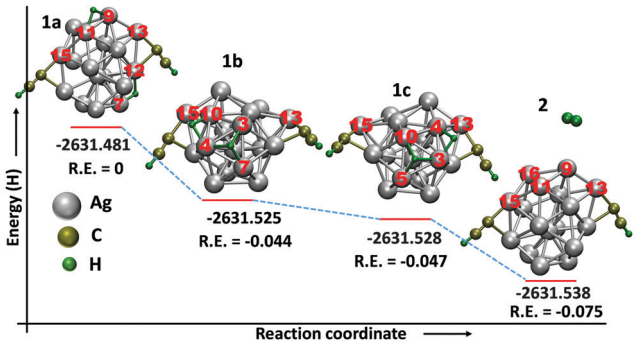

Fig. 4 Energy profile during the formation of $[Ag_{17}(C{\equiv}CH)_2]^+$ and a hydrogen molecule (**2**) starting from the intermediates (**1a–c**). During the optimization of the intermediate structure, there was mobility of bonded hydrogens with respect to silver atoms. The intermediates finally give the lower energy product after dehydrogenation. The total energy and relative energy values are in Hartree.

the surface of Ag_{17}^+. Here, like the previously reported $[Ag_7^+C_2H_2]$ cluster, we have also calculated a competitive isomer (**1a** in Fig. 4) of $[Ag_{17}(HC{\equiv}CH)_2]^+$, where one hydrogen from each of the acetylenes got dissociated and attached to the silver core transiently.[21] This competitive isomer was higher in energy (−2631.481 H) compared to the normal $[Ag_{17}(HC{\equiv}CH)_2]^+$ (−2631.588 H) and was consider as an intermediate structure for the next step. The attached hydrogens to silver, changed their positions with respect to the silver atoms during the optimization of the structure (**1a–c** in Fig. 4) and come out as a hydrogen molecule giving the final product, $[Ag_{17}(C{\equiv}CH)_2]^+$ (**2** in Fig. 4). The relatively lower energy of the product compared to the intermediates makes this reaction energetically favourable. Therefore, the formation of a hydrogen molecule is possible, which was observed in our experiments. Further detailed studies of binding of four and six acetylene molecules were also carried out which show the formation of hydrogen molecules and the products, $[Ag_{17}(C{\equiv}CH)_4]^+$ and $[Ag_{17}(C{\equiv}CH)_6]^+$, respectively (Fig. S19 and S20, ESI†). Energy profile of the overall reaction is shown in Fig. S21 (ESI†). The dehydrogenation process also has been calculated for an odd (one) number of acetylenes but it gives only a higher energy intermediate, and not any stable product (Fig. S22, ESI†). Therefore, dehydrogenation or formation of a hydrogen molecule was successful only when an even number of acetylenes interacted with Ag_{17}^+. The calculated binding energies after dehydrogenation are listed in Table S23 (ESI†). Calculated structures of $[Ag_{17}(C{\equiv}CH)]^+$ and $[C{\equiv}CH]$, generated during the CID experiment of $[Ag_{17}(C{\equiv}CH)_2]^+$ are shown in Fig. S24 (ESI†). Electronic structures of $[Ag_{17}(C{\equiv}CH)_2]^+$, $[Ag_{17}(C{\equiv}CH)]^+$ and $[C{\equiv}CH]$ have also been calculated and shown in Fig. S25–S27 (ESI†), respectively.

In conclusion, the naked cluster, Ag_{17}^+ was formed outside a mass spectrometer and for the first time, its reactivity with acetylene was studied around atmospheric pressure. During the reaction, dehydrogenation of acetylene results in the formation of acetylide attached Ag_{17}^+. Dehydrogenation occurred always for an even number of acetylenes, which also supports the dihydrogen molecule desorption. This study provides new insights into the binding mechanism of acetylene on Ag_{17}^+ and gives new light on the reactivity of size-selected naked clusters. As these reactions were conducted near ambient conditions, it is possible to collect the product on a suitable substrate for further characterization. Similar studies with other molecules may lead to new directions in gas phase clusters. Potential application of this method will be in the understanding of catalytic processes in atomically precise materials.

We thank the Department of Science and Technology for supporting our research. M. J. thanks U. G. C. for her SRF fellowship.

Conflicts of interest

There are no conflicts to declare.

Notes and references

1 I. Chakraborty and T. Pradeep, *Chem. Rev.*, 2017, **117**, 8208–8271.
2 J. Zhang, Z. Li, J. Huang, C. Liu, F. Hong, K. Zheng and G. Li, *Nanoscale*, 2017, **9**, 16879–16886.
3 M. Turner, V. B. Golovko, O. P. H. Vaughan, P. Abdulkin, A. Berenguer-Murcia, M. S. Tikhov, B. F. G. Johnson and R. M. Lambert, *Nature*, 2008, **454**, 981.
4 Z. Luo, A. W. Castleman and S. N. Khanna, *Chem. Rev.*, 2016, **116**, 14456–14492.
5 D. K. Boehme and H. Schwarz, *Angew. Chem., Int. Ed.*, 2005, **44**, 2336–2354.
6 S. M. Lang, T. M. Bernhardt, R. N. Barnett, B. Yoon and U. Landman, *J. Am. Chem. Soc.*, 2009, **131**, 8939–8951.
7 J.-M. Weibel, A. Blanc and P. Pale, *Chem. Rev.*, 2008, **108**, 3149–3173.
8 M. Meldal and C. W. Tornoe, *Chem. Rev.*, 2008, **108**, 2952–3015.
9 Z. Luo and A. W. Castleman, *Acc. Chem. Res.*, 2014, **47**, 2931–2940.
10 M. J. Manard, P. R. Kemper, C. J. Carpenter and M. T. Bowers, *Int. J. Mass Spectrom.*, 2005, **241**, 99–108.
11 W. Y. Lu, P. D. Kleiber, M. A. Young and K. H. Yang, *J. Chem. Phys.*, 2001, **115**, 5823–5829.
12 T. B. Ward, A. D. Brathwaite and M. A. Duncan, *Top. Catal.*, 2018, **61**, 49–61.
13 G. N. Khairallah and R. A. J. O'Hair, *Dalton Trans.*, 2007, 3149–3157, DOI: 10.1039/B700132K.
14 P. B. Armentrout, *Annu. Rev. Phys. Chem.*, 2001, **52**, 423–461.
15 M. Wleklinski, D. Sarkar, A. Hollerbach, T. Pradeep and R. G. Cooks, *Phys. Chem. Chem. Phys.*, 2015, **17**, 18364–18373.
16 M. Jash, A. C. Reber, A. Ghosh, D. Sarkar, M. Bodiuzzaman, P. Basuri, A. Baksi, S. N. Khanna and T. Pradeep, *Nanoscale*, 2018, **10**, 15714–15722.
17 A. Ghosh, M. Bodiuzzaman, A. Nag, M. Jash, A. Baksi and T. Pradeep, *ACS Nano*, 2017, **11**, 11145–11151.
18 A. Baksi, M. Jash, S. Bag, S. K. Mudedla, M. Bodiuzzaman, D. Ghosh, G. Paramasivam, V. Subramanian and T. Pradeep, *J. Phys. Chem. C*, 2019, **123**, 28494–28501.
19 M. S. Bootharaju, R. Dey, L. E. Gevers, M. N. Hedhili, J.-M. Basset and O. M. Bakr, *J. Am. Chem. Soc.*, 2016, **138**, 13770–13773.
20 M. Chen, J. E. Dyer, K. Li and D. A. Dixon, *J. Phys. Chem. A*, 2013, **117**, 8298–8313.
21 M. Yang, H. Wu, B. Huang and Z. Luo, *J. Phys. Chem. A*, 2019, **123**, 6921–6926.

